

Accurate feature extraction for multimodal biometrics combining iris and palmprint

Ritesh Vyas · Tirupathiraju Kanumuri ·
Gyanendra Sheoran · Pawan Dubey

Received: date / Accepted: date

Abstract Multimodal biometric systems provide a way to combat with the limitations of a unimodal biometric system which include less accuracy and user acceptability. In this context, a coding based approach called bit-transition code, is proposed for addressing the less-explored problem of designing a biometric-based authentication system by combining the iris and palmprint modalities. The approach is based on the encoding of binary transitions of symmetric and asymmetric parts of the Gabor filtered images at all pixel locations. Score-level fusion is employed to integrate the individual iris and palmprint performances. Experiments are carried out with three benchmark iris/palmprint databases, namely IITD iris and palmprint databases and PolyU palmprint database. The performance is measured in terms of receiver operator characteristics (ROC) curves and other metrics, like equal error rate (EER) and area under ROC curves (AUC). A comprehensive comparison, with several state-of-the-art approaches, is presented in order to validate the usefulness of the proposed approach.

Keywords Multimodal biometrics · iris recognition · palmprint recognition · bit-transition code

1 Introduction

Traditional ways of person authentication include knowledge based (like PIN and password) or token-based (like ID card and keys) approaches (Jain et al. 2004). But, these approaches are more vulnerable to security attacks like theft or password hacking (Lamiche et al. 2019). Therefore, a large interest

R. Vyas
Lancaster University, United Kingdom
E-mail: ritesh.vyas157@gmail.com

T. Kanumuri, G. Sheoran, P. Dubey
National Institute of Technology Delhi, India

has grown in biometric-based ways of authenticating an individual. The term biometrics refers to a pattern recognition approach which utilizes the distinctive features extracted from the physiological and/or behavioral attributes of humans, to establish their identities (Jain et al. 2007). Among all traits, iris and palmprint are two physiological traits which are known for their permanence, uniqueness and high recognition accuracy (Bowyer et al. 2008; Kong et al. 2009).

Biometric systems can be unimodal or multimodal depending upon whether single modality or multiple modalities are employed (Joseph et al. 2020). The unimodal biometric systems suffer from issues like spoof attacks, poor quality of samples, intra-class variations and user-acceptability (Modak and Jha 2019). These problems can be avoided to a large extent by combining information from different modalities (Tistarelli and Schouten 2011; Singh et al. 2019). Since, any biometric system should essentially have four basic modules (i.e. data acquisition, ROI segmentation, feature extraction, matching and decision modules), information fusion is possible at four different levels. Consequently, the fusion is classified as sensor-level fusion, feature-level fusion, score-level fusion and decision-level fusion (Saini and Sinha 2015; Lumini and Nanni 2017).

Sensor-level fusion contains the combination of raw data from different sensors or from different samples acquired with the same sensor. *Feature-level fusion* involves the combination of different set of features extracted from the input image, before storing them in a template. This fusion is subject to compatibility between different set of features. *Score-level fusion* fuses the scores obtained after application of different classifiers to same or different set of features. The final decision is made on the basis of combined scores. *Decision-level fusion* generally uses the match/non-match decision of different classifiers to derive a final decision. Whereas, *rank-level fusion* uses output from different biometric matchers to enhance the reliability of matching system. Among all types of fusion, score-level fusion is the most preferred one (Ross and Jain 2003; Hanmandlu et al. 2011).

Numerous efforts have been made till date to combine multiple biometric traits. Brunelli and Falavigna (1995) integrated acoustic and visual features to form a high-performance identification system. The speaker and face recognition systems were combined using measurement level and hybrid level integration. While, Hong and Jain (1998) combined the face and fingerprint modalities through decision-level fusion. Ben-Yacoub et al. (1999) evaluated different binary classifiers, like support vector machine (SVM) and multilayer perceptron, to attain the fusion of face and speech data.

Hanmandlu et al. (2011) used triangular norms (t-norms) for accomplishing score-level fusion of different modalities like palmprint, knuckle, hand-geometry and hand veins. Barra et al. (2014) presented a unified representation of matching scores and corresponding reliability of individual ear, face and iris traits. Barra et al. (2015) proposed fusion of electroencephalography (EEG) and electrocardiography (ECG) to develop a biometric system. Ahmad et al. (2016) employed non-stationary feature level fusion to combine face and

palmprint modalities. Hezil and Boukrouche (2017) performed feature-level fusion to combine the local features of ear and palmprint modalities.

However, there are very limited efforts from the research community to combine the two modalities of interest here, namely iris and palmprint. Kumar et al. (2010) proposed the use of adaptive combination strategies to find the optimal fusion strategy. Sun et al. (2014) proposed a linear programming based framework for ordinal feature selection of iris and palmprint. Wang et al. (2009) employed IrisCode and BLPOC based matching for iris and palmprint images, respectively, followed by score-level fusion through Gaussian mixture model. Additional details about the related works are presented in Table 1.

The limited availability of literature on combining iris and palmprint traits has prompted us to investigate the likelihood of their fusion. Moreover, the established fact that improvement due to data fusion is more prominent if the data being fused is more uncorrelated (Ross and Jain 2004), also plays the role of a key motivation behind the present study. Other advantages of exploiting iris and palmprint are that both these modalities offer high degrees of uniqueness. They are also able to distinguish the identical twins. Even left and right iris (or palmprint) of the same person are not alike. Moreover, both these modalities are said to be stable throughout one's life (Jain et al. 2004).

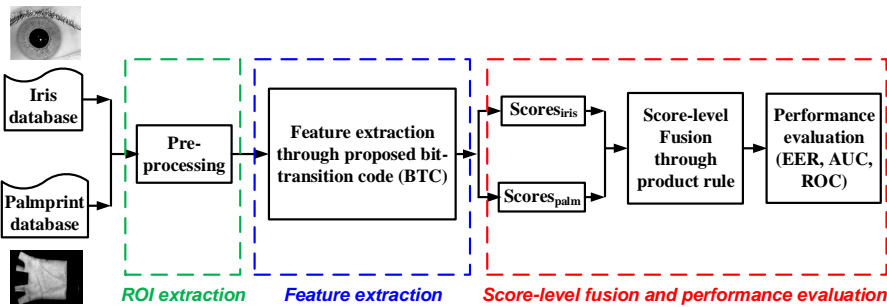


Fig. 1 Overall block diagram of the multimodal biometric system

This paper targets on designing a biometric system by presenting an effective feature representation scheme capable of retrieving meaningful features from both the iris and palmprint images. The overall block diagram for the concerned multimodal biometric system is depicted in Figure 1. This figure depicts the use of a single feature extraction scheme for both iris and palmprint. This scheme exploits the complementary information of real and imaginary Gabor responses by concatenating the zero-crossings of these responses into one vector. Thereafter, for each pixel location, a binary string is scanned across the dimension of concatenation and all 0-1 and 1-0 transitions are counted and stored in a matrix called bit-transition matrix. Elements of this matrix are then encoded to form the bit-transition codes. After forming the corresponding codes for both iris and palmprint databases, the matching is performed

Table 1 Details about related work

S.No.	Authors	Dataset	Fusion strategy	Performance metrics	Best values
1	Brunelli and Falavigna (1995)	Self-acquired face and voice database	Hybrid (rank+score level)	Correct identification rate	98%
2	Hong and Jain (1998)	MSU Fingerprint and public domain face database	Decision level	FRR (@FAR=1%)	1.80%
3	Ben-Yacoub et al. (?)	XM2VTS Database (images and synchronized speech)	SVM, Fisher's LDA, MLP	EER	0.6
4	Hanmandlu et al. (2011)	IITD (Hand Geometry) PolyU (Knuckle and palmprint)	Triangular norms	GAR (@FAR=0.01%)	100%
5	Barra et al. (2014)	Notre Dame Ear database AR-Faces database UBIRIS-v1	Complex fusion	Recognition rate (RR) EER	1.00, 0.028
6	Barra et al. (2015)	Self-acquired EEG and ECG database	K-means clustering followed by grouping of centroids	EER	2.94
7	Ahmad et al. (2016)	ORL and FERET face databases PolyU palmprint database	Non-stationary feature fusion	Recognition accuracy	99.70%
8	Hezil and Boukrouche (2017)	IIT-Delhi-2 Ear database IITD touchless palmprint database	Canonical correlation analysis (CCA) and series feature fusion	Correct recognition rate	100%
9	Kumar et al. (2010)	IITD Iris PolyU Palmprint XM2VTS Face and speech database FVC 2004	Score and decision level fusion (hybrid PSO)	ROC and score-distribution curves	—
10	Wang et al. (2009)	CASIA Iris and PolyU palmprint database	Gaussian Mixture Model (GMM) with score normalization	EER	1.75%

to obtain the genuine and imposter scores. Subsequently, score-level fusion is employed to achieve improved performance metrics.

The organization of the paper is as follows. Section 2 provides the details about ROI segmentation of iris and palmprint images. While, Section 3 details the proposed feature extraction approach. Details of experimental setup and results are presented in Section 4. Finally, the paper is concluded in Section 5.

2 ROI segmentation

Segmentation of region of interest (ROI) from the acquired image is one of the vigorous components of any biometric system. It plays an important role in extraction of more reliable features. The accuracy of the segmentation module directly affects the overall system accuracy. In this work, the segmentation of iris and palmprint is achieved through the methods given in Vyas et al. (2017) and Zhang et al. (2003), respectively.

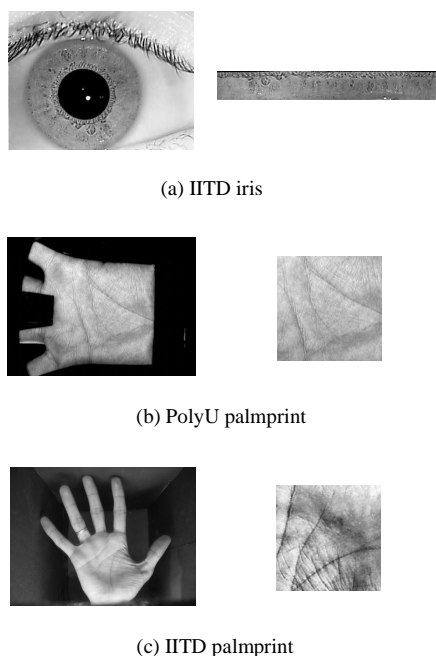


Fig. 2 Sample raw and segmented images from the employed databases

The segmentation of pupillary boundary (the boundary between iris and pupil) is achieved by exploiting its property to be most dark and most connected region of a standard eye image. Whilst, the limbic boundary (the boundary between iris and sclera) is localized through formation of an adaptive

mask, which is found to be less affected by the non-significant regions like eyelashes/eyelids. On the other hand, the segmented regions-of-interest (ROI's) for the palmprint modality are provided with the databases themselves. However, it is eminent that the palmprint region can be readily localized by spotting the finger-valley points and extracting the region falling normal to the line joining those valley points. The readers are directed to the aforementioned references for more details on the segmentation procedures. The image samples and corresponding ROI images are illustrated in Figure 2.

3 Proposed feature extraction approach

The proposed approach is based on the counting of bit transitions in a binary string formed from the concatenated vectors of binarized real and imaginary parts of Gabor filtered iris and palmprint images. Initially, the iris/palmprint image is processed through Wiener filter and histogram equalization to highlight the critical textural regions. The Wiener filter is employed to remove the effects of noise (Zuo and Schmid 2010), like blur (majorly occurring due to linear motion). Thereafter, HAAR decomposition is employed to restrain the feature vector size and speed-up the computations (Tamrakar and Khanna 2015). Moreover, HAAR wavelet yields the approximation of image details in prominent directions like horizontal, vertical and diagonal (Alonso-Fernandez and Bigun 2016). The decomposed image is then filtered through 2D Gabor filters, with varying spatial frequencies and orientations (chosen from Kong et al. (2003)), in order to behold the textural properties of both the iris and palmprint images. A set of experiments is performed to obtain the ideal set of filter parameters. This rigorous experimentation leads to the empirical selection of Gabor parameters, such as the scale and frequency are chosen as 5.6180 and 0.0916, respectively. The number of orientations is fixed to five for both the iris and palmprint images. Whereas, size of the Gabor filter is selected as 15×15 and 31×31 for iris and palmprint images, respectively. This variation in filter sizes is adapted to cater with the micro and macro features of iris and palmprint images, respectively, e.g. presence of small-scale texture regions in iris and relatively large-scale palm lines in palmprint.

After filtering, the symmetric and anti-symmetric parts of the output images are binarized through zero-crossing operation and concatenated across the third dimension of the matrix, as both these parts are said to pursue different information (Kumar and Pang 2002). Thereafter, concatenation of binarized real and imaginary Gabor responses is performed. It is because of this concatenation that the texture variations of iris image can be captivated by scanning in the direction of concatenation. The binary string formed after this scanning is used further in the encoding stage. The number of bit-transitions (i.e. '0' to '1' and '1' to '0' changes) in this binary string is used for corresponding texture representation resulting into a bit-transition matrix. Further, encoding of bit-transition matrix is done in order to form the bit-transition code (BTC). The proposed feature extraction process is illustrated in Algorithm 1.

Algorithm 1 Proposed feature extraction (BTC)**Require:** I : Iris/Palmprint ROI image**Ensure:** btc : bit-transition code planes1: Apply preprocessing steps to I .2: Obtain the decomposed version of I into I_1 .

3: Design 2D Gabor filters as per following equation:

$$G_n(x, y, \sigma, f) = \frac{1}{\sqrt{2\pi\sigma^2}} \exp\left\{-\frac{x^2 + y^2}{\sigma^2}\right\} \times \exp(2\pi i f (x \cos \theta + y \sin \theta)) \quad \triangleright \text{ where,}$$

$\theta = \frac{n\pi}{N}$, $0 \leq n \leq N - 1$, N being the total number of orientations, σ and f represent scale and frequency, respectively, $(x, y) \in W$, W being the filter's window size.

4: **for** $n = 0$ to $N - 1$ **do**5: Filter I_1 with 2D Gabor filter through convolution operation: $\bar{I}_{1,n} = I_1 * G_n$ 6: $\bar{I}_{1,n,r} = \text{Re}(\bar{I}_{1,n})$, $\bar{I}_{1,n,i} = \text{Im}(\bar{I}_{1,n})$ 7: At each pixel (x, y) , evaluate

$$\bar{I}_{1,n,r}^{new}(x, y) = \begin{cases} 1, & \text{if } \bar{I}_{1,n,r}(x, y) > 0 \\ 0, & \text{otherwise} \end{cases}$$

$$\bar{I}_{1,n,i}^{new}(x, y) = \begin{cases} 1, & \text{if } \bar{I}_{1,n,i}(x, y) > 0 \\ 0, & \text{otherwise} \end{cases}$$

8: Concatenation:

$$M(x, y, 2 * n + 1) = \bar{I}_{1,n,r}^{new}(x, y)$$

$$M(x, y, 2 * n + 2) = \bar{I}_{1,n,i}^{new}(x, y)$$

9: **end for**10: **for** each pixel (x, y) **do**11: **for** $i = 1$ to $2N$ **do**12: $s(i) = M(x, y, i)$ 13: **end for**14: **for** $j = 1$ to $2N-1$ **do**15: $temp(j) = s(j) - s(j + 1)$ 16: **end for**17: $S(x, y) = \#(temp \neq 0)$ \triangleright where $\#(temp \neq 0)$ is the total count of $temp$ which is non-zero and S is the bit-transition matrix.18: **end for**19: **for** $p = 1$ to $\left\lceil \frac{2N + 1}{2} \right\rceil$ **do**20: $btc(x, y, p) = \begin{cases} 1, & p \leq S(x, y) < p + \frac{N + 1}{2} \\ 0, & \text{otherwise} \end{cases}$ 21: **end for**22: **return** btc

For more clear depiction of the proposed feature extraction process, Figure 3 shows the outcome images of each of the employed steps. The figure shows two parallel frameworks, namely iris and palmprint, along with the prominent step written on their left side. The preprocessing of ROI images is employed to accomplish the embossing of prominent texture regions, in order to enhance their likelihood of being captured. Subsequently, the preprocessed image is decomposed. Interestingly, it can be observed from Figure 3 that decomposition reduces the size of ROI image and accelerates the whole feature extraction process, while retaining the crucial features at the same time. Afterwards, the decomposed image is filtered through 2D Gabor filters, with varying orientations, so that wide-ranging texture residing in the iris/palmprint images can

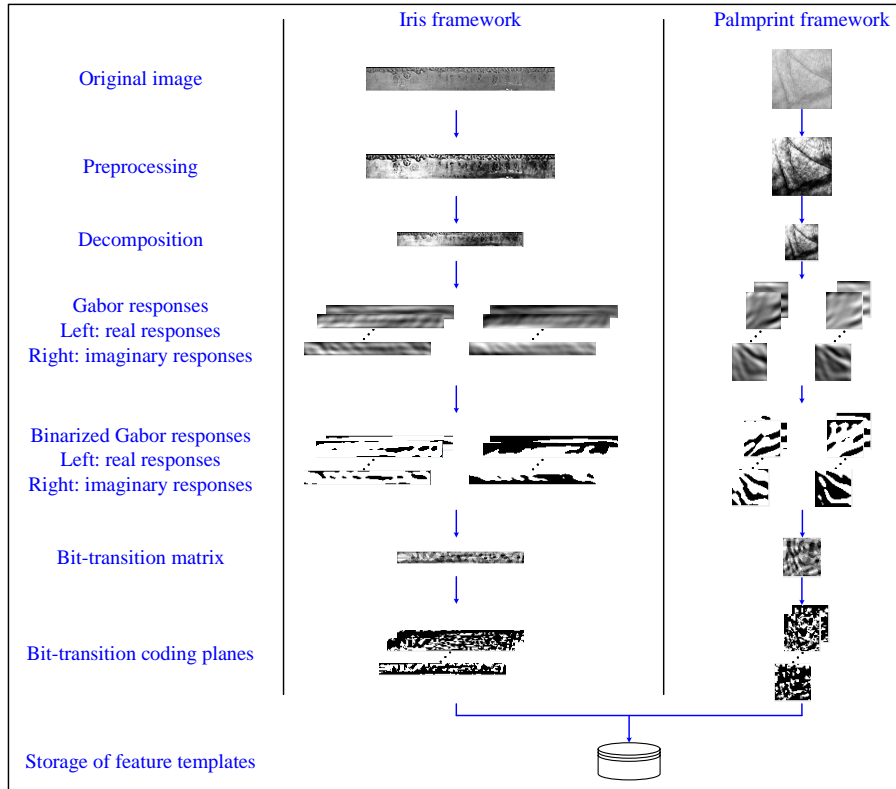


Fig. 3 Pictorial demonstration of the proposed approach

be consisted in the final feature vector. Figure 3 shows the real and imaginary parts of the Gabor filtered images for five different orientations.

Consequently, the filter responses are binarized using zero crossing. This step reveals which part of the texture region is obtained under which orientation of the Gabor filter. The binarized real and imaginary responses are then placed side-by-side and number of bit-transitions are counted at each spatial location. This count value is then stored in a matrix, called bit-transition matrix. Elements of this bit-transition matrix (denoted by ‘ S ’ in Algorithm 1) can overtly take values between ‘0’ and ‘ $2N - 1$ ’, where ‘ N ’ corresponds to the number of orientations of employed Gabor filters. After this, the bit-transition matrix is encoded into bit-planes as explained in Algorithm 1. Finally, the encoded bit-planes from iris and palmprint frameworks are stored in a template database, as illustrated in Figure 3.

3.1 Matching

In order to calculate the distance between the query and gallery image feature vectors, matching has to be performed. Since the proposed feature extraction approach generates binary features, the distance metric employed in this work is the Hamming distance, defined as follows:

$$Dist(Q, G) = \frac{\sum_{x=1}^X \sum_{y=1}^Y \sum_{p=1}^P btc_Q(x, y, p) \oplus btc_G(x, y, p)}{X \times Y \times P} \quad (1)$$

where, X, Y are the dimensions of the feature vectors, P represents the number of bit-planes in btc and \oplus indicates the ‘XOR’ operation between p^{th} bit-planes of the feature vectors. btc_Q and btc_G represent the extracted feature vectors for the query and gallery sample, respectively.

3.2 Score-level fusion

Among all the fusion stages, score-level fusion is the most preferred one. Reasons behind the popularity of score-level fusion are ease in the calculation of scores and presence of adequate distinctive information in the scores (He et al. 2010). Moreover, scores can be fused without any knowledge of the foregoing feature extraction and matching algorithms. Different scores for M different modalities i.e. S_1, S_2, \dots, S_M can be combined to get one score vector S using a function F as follows:

$$S = F(S_1, S_2, \dots, S_M) \quad (2)$$

In this study, the function F is selected as per the product rule of fusion, as this rule is empirically proven to be outperforming other popular rules of fusion, namely minimum, maximum and Sum rules. Mathematically, the product rule of fusion can be illustrated as follows:

$$S = \prod_{i=1}^M S_i \quad (3)$$

4 Experimental setup and results

4.1 Databases

The fusion of iris and palmprint modalities is tested on two multimodal databases, namely Multimodal Database-1 (MMDB1) and Multimodal Database-2 (MMDB2), prepared by merging three popular publicly available databases:

IIT Delhi iris database¹, PolyU palmprint database² and IIT Delhi Touchless Palmprint Database (Version 1.0)³ database. Hence, the databases are chimeric (Nigam and Gupta 2015) and follow the property of no correlation between the chosen modalities. Notably, the databases are chimeric in the sense that samples of individual iris and palmprint traits are taken from three different datasets (Barra et al. 2014). The IITD iris database contains 2240 images from 224 different subjects i.e. 5 images from the left eye and 5 from the right eye. The PolyU II version palmprint database is acquired from 386 different palms in two separate sessions, capturing around 10 images per palm in each session. The IITD palmprint database was acquired using a touchless imaging setup from 235 volunteers at IIT Delhi.

The first multimodal database used in this work, termed as MMDB1, is formed by merging 500 images each from IITD iris and PolyU palmprint databases, at a rate of 5 images per iris/palm. Whereas, the second database, MMDB2, is created by merging 500 images each from IITD iris and palmprint databases. Now, both multimodal databases are said to have 1000 images from 100 iris and palms. During matching phase, each iris/palm image of one database is matched against all other iris/palm images in that database. Consequently, $100 \times {}^5C_2$ (= 1000) genuine and ${}^{100}C_2 \times 5^2$ (= 123750) imposter scores are generated. All the generated scores are indeed distance scores which means their lower values exhibit better match among the samples. In addition to that, the scores for iris and palmprint modalities fall in the same range of [0,1], hence excluding the need of any type of score normalization. The scores from iris and palmprint modalities are then fused to obtain combined performance of the multimodal system. The performance is evaluated in terms of different metrics like false acceptance rate (FAR), false rejection rate (FRR), genuine acceptance rate (GAR), equal error rate (EER) and area under receiver operator characteristics (ROC) curves. The ROC curves for different modalities using different feature extraction schemes are then plotted to observe the trade-off between the threshold and the FAR/FRR values.

The superiority of the proposed approaches is established through its comparison with several benchmark approaches. In order to make this comparison more suggestive, only those state-of-the-art approaches are selected which yield reasonable accuracies for both iris and palmprint. Subsequently, the proposed approach is compared with following benchmark approaches, band-limited phase only correlation (BLPOC) (Koichi et al. 2006; Miyazawa et al. 2008), XorSum Code (Tamrakar and Khanna 2015; Vyas et al. 2016), Zernike moments (ZM) (Badrinath et al. 2011; Tan and Kumar 2014), difference of variance (DoV) (Vyas et al. 2019), Log-Gabor filter (Masek 2003) and Haralick features (Subban et al. 2018, Latha and Prasad 2015). **All the feature**

¹ available at http://www4.comp.polyu.edu.hk/~csajaykr/IITD/Database_Iris.htm, last accessed on September 22, 2020

² available at <http://www4.comp.polyu.edu.hk/~biometrics/>, last accessed on September 22, 2020

³ available at http://www4.comp.polyu.edu.hk/~csajaykr/IITD/Database_Palm.htm, last accessed on September 22, 2020

descriptors employed in this paper are implemented on the same experimental setup as that of the proposed approach. It is worth mentioning that matching of Haralick features is accomplished through chi-square distance measure. Furthermore, implementation of BLPOC, XorSum and DoV approaches is completed with the parameters reported in their respective references. Whereas, in implementation of ZM, the order and repetition number of Zernike moment is taken as one. The detailed discussion about the results achieved in the proposed approach as well as in the aforementioned approaches is given in the following subsection.

4.2 Results and discussion

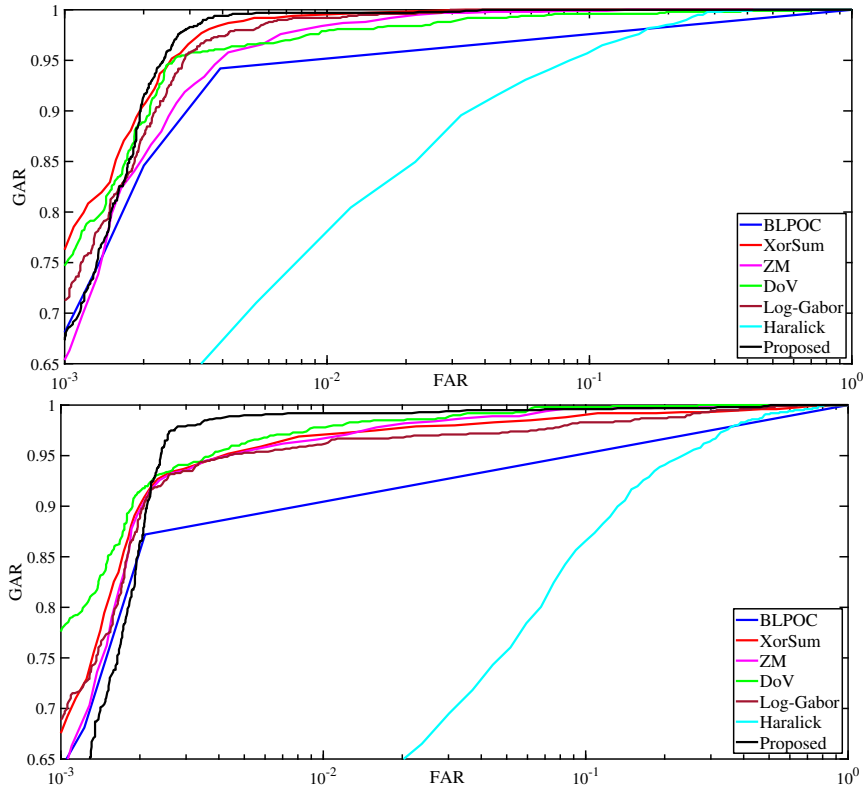
The performance metrics for the proposed approach as well as for the state-of-the-art approaches are presented in Tables 2 and 3. Table 2 provides the EER and AUC values for individual iris and palmprint modalities. While, Table 3 corresponds to the metrics of the considered multimodal databases. It can be noticed from Table 2 that the proposed approach generates considerable metrics (EER and AUC) for both iris and palmprint modalities individually. This table clearly validates the fact that the proposed approach is equally effective in representing the iris and palmprint images. For instance, EER and AUC of the proposed approach for IITD iris database is 1.60% and 99.67%, respectively, which surpass their counterpart values produced with other state-of-the-art approaches. On the other hand, performance of the proposed approach for PolyU and IITD palmprint databases are comparable to the state-of-the-art approaches. In fact, for PolyU palmprint, the proposed approach yields second best EER after XorSum. Notably, the individual performances of all the approaches for IITD palmprint images are relatively poor, which can be regarded as the impact of large intra-class variations in the images of this database owing to its touchless acquisition setup.

Table 2 Performance metrics (%) for unimodal scenario

Modality	Iris		Palmprint (PolyU)		Palmprint (IITD)	
	EER	AUC	EER	AUC	EER	AUC
BLPOC	3.82	98.23	8.45	95.98	22.72	86.58
XorSum	2.22	99.56	7.76	97.50	19.22	88.33
ZM	4.20	99.11	9.08	96.09	16.07	90.45
DoV	4.88	98.84	8.21	96.72	10.52	95.69
Log-Gabor	1.98	99.49	9.47	95.30	19.15	87.52
Haralick	13.76	93.93	14.54	92.43	27.12	80.20
Proposed	1.60	99.67	8.01	96.36	19.24	87.48

Table 3 Performance metrics (%) for multimodal scenario

Modality	MMDB1		MMDB2	
	EER	AUC	EER	AUC
BLPOC	3.10	97.02	6.50	93.54
XorSum	0.67	99.93	2.18	99.42
ZM	1.23	99.86	1.92	99.73
DoV	1.67	99.73	1.53	99.84
Log-Gabor	0.80	99.91	2.92	99.32
Haralick	6.47	98.50	11.68	95.37
Proposed	0.42	99.92	0.81	99.75

**Fig. 4** Comparative ROC curves for (top) MMDB1, (bottom) MMDB2

Considering the performance for multimodal databases (Table 3), it can be firmly stated that the proposed approach is generating promising results, outperforming every other benchmark approach. EER and AUC of the proposed approach for MMDB1 database are obtained as 0.42% and 99.92%, respectively. These values are apparently in line with the rich textural details being

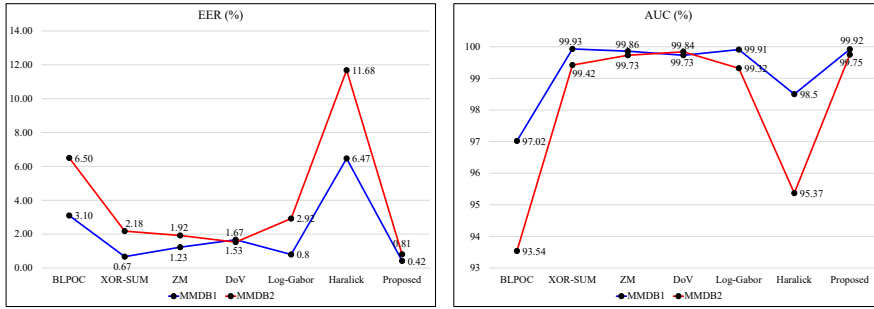


Fig. 5 Comparative line charts; (left) EER comparison, (right) AUC comparison

captured by the proposed feature descriptor. Additionally, the comparative ROC curves shown in Figure 4 (top) explains the outperforming nature of the proposed descriptor. More importantly, the ROC curve of the proposed approach is covering a larger area, owing to its adequate feature representation. In a similar fashion, the proposed descriptor yields EER and AUC of 0.81% and 99.75%, respectively, for the MMDB2 database. Since MMDB2 comprises of palmprint images from IITD palmprint database, it offers huge challenge in terms of mitigating the effect of vast intra-class variations. Still, the proposed descriptor is producing interesting results e.g. 0.81% EER having approximately 47% improvement over the second best approach. Besides, ROC of the proposed descriptor for MMDB2 database is clearly depicting its remarkable performance (kindly refer to Figure 4(bottom)).

In addition to the above, Figure 5 is plotted to show clear comparison between EER (Figure 5(left)) and AUC (Figure 5(right)) values of all the concerned approaches, in the form of line charts. These line charts give a better view to the reader for deducing the exceptional performance of the proposed descriptor for both chimeric multimodal databases considered in this work. Moreover, the genuine acceptance rate (GAR) of the concerned multimodal biometric system at low FAR of, say 0.5%, is recorded as 99.6% and 99%, respectively, for MMDB1 and MMDB2.

5 Conclusion

In this paper, combination of iris and palmprint biometric modalities is explored. An efficient approach, called bit-transition code, is proposed for the scenario of multimodal biometric system. The approach starts with filtering of the input images with Gabor filter yielding complex responses. Thereafter, real and imaginary parts of the complex responses are binarized through zero-crossing and concatenated alongside. This task continues for all employed orientations of the Gabor filter. Thereafter, a binary string is formed by scanning the concatenated vector along the dimension of concatenation and number of

bit-transitions in that binary string are encoded to form the bit-transition codes. Investigation of different performance metrics and an exhaustive comparison confirm that the proposed approach performs at par for concerned multimodal biometric framework, with EER as low as 0.4-0.8 % and AUC as high as 99.7-99.9 %.

Acknowledgements The authors wish to thank Indian Institute of Technology, Delhi and The Hong Kong Polytechnic University, Hong Kong for providing free access to their iris and palmprint databases.

References

- Ahmad MI, Woo WL, Dlay S (2016) Non-stationary feature fusion of face and palmprint multimodal biometrics. *Neurocomputing* 177:49–61
- Alonso-Fernandez F, Bigun J (2016) A survey on periocular biometrics research. *Pattern Recognition Letters* 82:92–105
- Badrinath GS, Kachhi NK, Gupta P (2011) Verification system robust to occlusion using low-order Zernike moments of palmprint sub-images. *Telecommun Syst* 47(3-4):275–290
- Barra S, De Marsico M, Nappi M, Riccio D (2014) Complex numbers as a compact way to represent scores and their reliability in recognition by multi-biometric fusion. *International Journal of Pattern Recognition and Artificial Intelligence* 28(07):1460003
- Barra S, Casanova A, Frascini M, Nappi M (2015) EEG/ECG signal fusion aimed at biometric recognition. In: *International Conference on Image Analysis and Processing*, Springer, pp 35–42
- Ben-Yacoub S, Abdeljaoued Y, Mayoraz E (1999) Fusion of face and speech data for person identity verification. *IEEE Trans Neural Networks* 10(5):1065–1074
- Bowyer KW, Hollingsworth K, Flynn PJ (2008) Image understanding for iris biometrics: A survey. *Comput Vis Image Underst* 110(2):281–307
- Brunelli R, Falavigna D (1995) Person identification using multiple cues. *IEEE Trans Pattern Anal Mach Intell* 17(10):955–966
- Hanmandlu M, Grover J, Gureja A, Gupta HM (2011) Score level fusion of multimodal biometrics using triangular norms. *Pattern Recognit Lett* 32(14):1843–1850
- He M, Horng SJ, Fan P, Run RS, Chen RJ, Lai JL, Khan MK, Sentosa KO (2010) Performance evaluation of score level fusion in multimodal biometric systems. *Pattern Recognit* 43(5):1789–1800
- Hezil N, Boukrouche A (2017) Multimodal biometric recognition using human ear and palmprint. *IET Biometrics* 6(5):351–359
- Hong L, Jain A (1998) Integrating faces and fingerprints for personal identification. *IEEE Trans Pattern Anal Mach Intell* 20(12):1295–1307
- Jain AK, Ross A, Prabhakar S (2004) An Introduction to biometric recognition. *IEEE Trans Circuits Syst Video Technol* 14(1):4–20

- Jain AK, Flynn P, Ross AA (2007) Handbook of biometrics. Springer Science & Business Media
- Joseph T, Kalaiselvan SA, Aswathy SU, Radhakrishnan R, Shamna AR (2020) A multimodal biometric authentication scheme based on feature fusion for improving security in cloud environment. *Journal of Ambient Intelligence and Humanized Computing* pp 1–9
- Koichi I, Aoki T, Nakajima H, Kobayashi K, Higuchi T (2006) A palmprint recognition algorithm using phase-based image matching. In: IEEE Int. Conf. Image Process., 2, pp 2669–2672
- Kong A, Zhang D, Kamel M (2009) A survey of palmprint recognition. *Pattern Recognit* 42(7):1408–1418
- Kong WK, Zhang D, Li W (2003) Palmprint feature extraction using 2-D Gabor filters. *Pattern Recognit* 36(10):2339–2347
- Kumar A, Pang GK (2002) Defect detection in textured materials using gabor filters. *IEEE Trans Ind Appl* 38(2):425–440
- Kumar A, Kanhangad V, Zhang D (2010) A new framework for adaptive multimodal biometrics management. *IEEE Transactions on Information Forensics and Security* 5(1):92–102
- Lamiche I, Bin G, Jing Y, Yu Z, Hadid A (2019) A continuous smartphone authentication method based on gait patterns and keystroke dynamics. *Journal of Ambient Intelligence and Humanized Computing* 10(11):4417–4430
- Latha YM, Prasad MV (2015) GLCM based texture features for palmprint identification system. In: *Computational Intelligence in Data Mining*—Volume 1, Springer, pp 155–163
- Lumini A, Nanni L (2017) Overview of the combination of biometric matchers. *Inf Fusion* 33:71–85
- Masek L (2003) Recognition of human iris patterns for biometric identification. PhD thesis, University of Western Australia
- Miyazawa K, Ito K, Aoki T, Kobayashi K, Nakajima H (2008) An effective approach for Iris recognition using phase-based image matching. *IEEE Trans Pattern Anal Mach Intell* 30(10):1741–1756
- Modak SKS, Jha VK (2019) Multibiometric fusion strategy and its applications: A review. *Information Fusion* 49:174–204
- Nigam A, Gupta P (2015) Designing an accurate hand biometric based authentication system fusing finger knuckleprint and palmprint. *Neurocomputing* 151:1120–1132
- Ross A, Jain A (2003) Information fusion in biometrics. *Pattern Recognit Lett* 24(13):2115–2125
- Ross A, Jain AK (2004) Multimodal biometrics : an overview. In: *12th European Signal Processing Conference (EUSIPCO)*, pp 1221–1224
- Saini N, Sinha A (2015) Face and palmprint multimodal biometric systems using Gabor–Wigner transform as feature extraction. *Pattern Analysis and Applications* 18(4):921–932
- Singh M, Singh R, Ross A (2019) A comprehensive overview of biometric fusion. *Information Fusion* 52:187–205

- Subban R, Susitha N, Mankame DP (2018) Efficient iris recognition using Haralick features based extraction and fuzzy particle swarm optimization. *Cluster Computing* 21(1):79–90
- Sun Z, Wang L, Tan T (2014) Ordinal feature selection for iris and palmprint recognition. *IEEE Transactions on Image Processing* 23(9):3922–3934
- Tamrakar D, Khanna P (2015) Palmprint verification with XOR-SUM Code. *Signal, Image Video Process* 9:535–542
- Tan CW, Kumar A (2014) Accurate iris recognition at a distance using stabilized iris encoding and Zernike moments phase features. *Image Process IEEE Trans* 23(9):3962–3974
- Tistarelli M, Schouten B (2011) Biometrics in ambient intelligence. *Journal of Ambient Intelligence and Humanized Computing* 2(2):113–126
- Vyas R, Kanumuri T, Sheoran G (2016) Iris recognition using 2-D Gabor filter and XOR-SUM Code. In: *IEEE India Int. Conf. Image Process.*
- Vyas R, Kanumuri T, Sheoran G (2017) Non-parametric iris localization using pupil’s uniform intensities and adaptive masking. In: *2017 IEEE Annual India Conference (INDICON)*, pp 1–4
- Vyas R, Kanumuri T, Sheoran G (2019) Cross spectral iris recognition for surveillance based applications. *Multimedia Tools and Applications* 78(5):5681–5699
- Wang J, Li Y, Ao X, Wang C, Zhou J (2009) Multi-modal biometric authentication fusing iris and palmprint based on GMM. In: *2009 IEEE/SP 15th Workshop on Statistical Signal Processing*, IEEE, pp 349–352
- Zhang D, Kong WK, You J, Wong M (2003) Online palmprint identification. *IEEE Trans Pattern Anal Mach Intell* 25(9):1041–1050
- Zuo J, Schmid Na (2010) On a methodology for robust segmentation of non-ideal iris images. *IEEE Transactions on Systems, Man, and Cybernetics, Part B: Cybernetics* 40(3):703–718